joining triad, and assignments are possible by inspection. Narrowest ^{183}W NMR lines result from the broadest ^{51}V resonances which in turn stem from high-viscosity solutions at low temperature.

Finally, 2-D ^{51}V J-correlation spectroscopy (COSY) extends the concept of measuring metal–metal atom connectivity patterns to quadrupolar nuclei. Although not all possible connections are observed due to the small magnitude of $^2J_{V-O-V}$ relative to T_2^{-1}, adjacent locations in the Keggin structure are easily detectable. These data complement ^{183}W–^{183}W atom connectivities and will prove to be a useful structural tool in higher vanadium substituted species.

Acknowledgment. I am grateful to Professor M. T. Pope and M. Leparulo for sharing information and providing a sample of $[SiV^{IV}_2W_{10}O_{40}]^{8-}$ for comparison with our compounds. Professor R. G. Finke and B. Rapko kindly supplied details of their synthesis of β-$[SiV_3W_9O_{40}]^{7-}$. I also thank W. H. Knoth for stimulating discussions. G. Watunya, J. Jensen, and J. T. Seningen provided skilled technical assistance.

Saturated and Polymerizable Amphiphiles with Fluorocarbon Chains. Investigation in Monolayers and Liposomes

R. Elbert, T. Folda, and H. Ringsdorf*

Contribution from the Institute of Organic Chemistry, University of Mainz, D-6500 Mainz, Federal Republic of Germany. *Received March 6, 1984*

Abstract: The synthesis and characterization of several saturated and polymerizable amphiphiles with fluorocarbon chains are described. Monolayers of lipids containing fluorocarbon chains are more stable than those formed from their hydrocarbon counterparts. The creation of phase-separated monolayers and liposomes is possible when the membrane is composed of a mixture of lipids containing hydrocarbon chains and lipids containing fluorocarbon chains. Phase separation even occurs when the two lipids bear the same head group. Complete phase separation of a natural lipid (DMPC) and a lipid with fluorocarbon chains, **1**, could be demonstrated in liposomes by using freeze-fracture electron microscopy. Phase separation was even confirmed when the percentage of the fluorocarbon amphiphile was as low as 5 mol %. The polymerization behavior of unsaturated amphiphiles with fluorocarbon chains was investigated in monolayers and liposomes. The polymerization in liposomes could be followed by UV spectroscopy. Preservation of the spherical structure of the polymeric vesicles is demonstrated by electron microscopy.

Monolayers, black lipid membranes, and liposomes from natural and synthetic lipids are of interest as models for biological membranes. In addition, the polymerization of lipid molecules containing 1,3-butadiyne,[1-3] butadiene,[4] methacrylate, or acrylate[4-6] moieties as polymerizable groups leads to more stable model membranes. Nearly all amphiphiles investigated so far in this connection contain hydrocarbon chains as a hydrophobic moiety.

Perfluorocarbons are known to have physical properties which differ from their hydrocarbon analogues and often are immiscible with hydrocarbons.[7,8] Tensids containing fluorocarbon chains are known to have critical micelle concentrations similar to comparable hydrocarbon surfactants containing a 50% longer alkyl chain.[9] The greater hydrophobicity of a CF_2 group compared to a CH_2 group and the limited miscibility of fluorocarbon and hydrocarbon amphiphiles in micelles[10] were the reasons for the recent investigation of liposome-forming amphiphiles containing fluorocarbon chains.[11]

In this publication the synthesis of both saturated and polymerizable fluorine-containing amphiphiles and their behavior in monolayers and liposomes are described. As in the case of hydrocarbon lipids, the polymerization of fluorocarbon amphiphiles could be expected to enhance the stability of such model membranes. The mixing behavior of lipids with hydrocarbon and

Table I. Structure and Melting Points of Fluorocarbon and Hydrocarbon Amphiphiles

no.	compound	melting point, °C
1	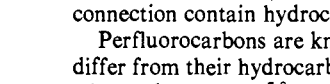	38
2	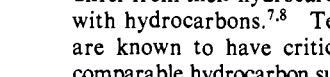	124
3	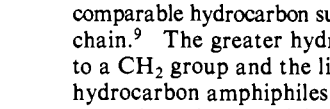	160–161
4	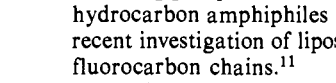	116
5	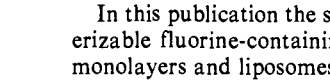	142[23]
6	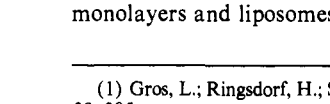	108
7	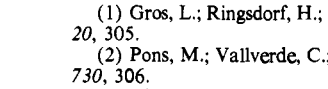	49
8	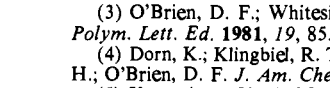	66
9	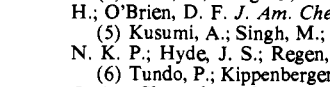	88[25]
10	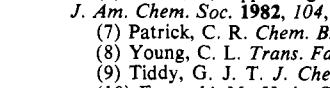	79–80

(1) Gros, L.; Ringsdorf, H.; Schupp, H. *Angew. Chem. Int. Ed. Engl.* **1981**, *20*, 305.
(2) Pons, M.; Vallverde, C.; Chapman, D. *Biochim. Biophys. Acta* **1983**, *730*, 306.
(3) O'Brien, D. F.; Whitesides, T. H.; Klingbiel, R. T. *J. Polym. Sci., Polym. Lett. Ed.* **1981**, *19*, 85.
(4) Dorn, K.; Klingbiel, R. T.; Specht, D. P.; Tyminski, P. N.; Ringsdorf, H.; O'Brien, D. F. *J. Am. Chem. Soc.* **1984**, *106*, 1627.
(5) Kusumi, A.; Singh, M.; Tirrell, D. A.; Oehme, G.; Singh, A.; Samuel N. K. P.; Hyde, J. S.; Regen, S. L. *J. Am. Chem. Soc.* **1983**, *105*, 2975.
(6) Tundo, P.; Kippenberger, D. J.; Politi, M. J.; Klahn, P.; Fendler, J. H. *J. Am. Chem. Soc.* **1982**, *104*, 5352.
(7) Patrick, C. R. *Chem. Br.* **1971**, *7*, 154.
(8) Young, C. L. *Trans. Faraday Soc.* **1969**, *65*, 2639.
(9) Tiddy, G. J. T. *J. Chem. Soc., Faraday Trans. 1*, **1972**, *68*, 369.
(10) Funasaki, N.; Hada, S. *J. Phys. Chem.* **1980**, *84*, 1868.
(11) Kunitake, T.; Okahata, Y.; Yasunami, S. *J. Am. Chem. Soc.* **1982**, *104*, 5547.

0002-7863/84/1506-7687$01.50/0

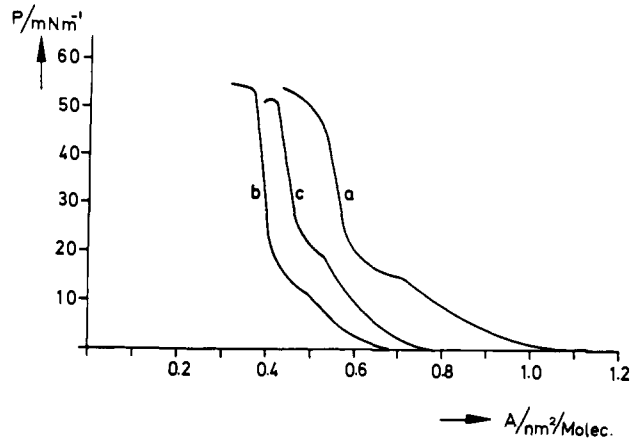

Figure 1. Surface pressure–area diagrams of **1** (a), **2** (b), and **3** (c) at 20 °C (subphase: H_2O).

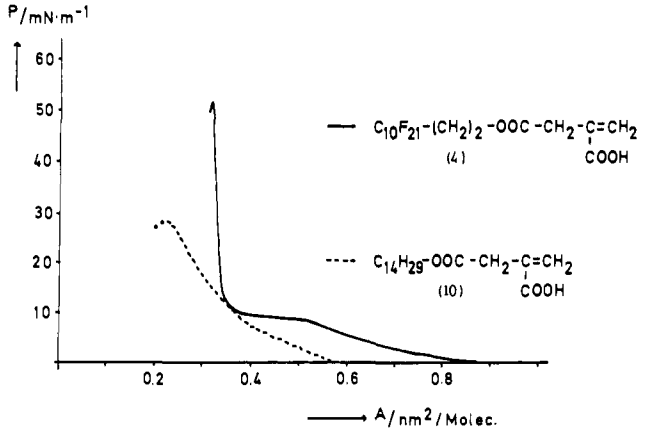

Figure 2. Surface pressure–area diagrams of **4** and **10** at 20 °C (subphase: H_2O).

fluorocarbon chains in monolayers and in liposomes was also investigated.

Results and Discussion

Saturated and polymerizable fluorocarbon amphiphiles containing different polymerizable groups were synthesized, **1–6**. Analogous hydrocarbon amphiphiles **7–10** were prepared for use in comparison investigations and for miscibility studies. The structures and melting points of the amphiphiles are given in Table I.

Monolyaer Properties of Fluorocarbon Amphiphiles. The amphiphiles **1–6** form monolayers at the gas/water interface. The surface pressure–area diagrams of **1–3** are displayed in Figure 1. These diagrams show the dependence of the spreading behavior on the head group of the amphiphile.

At 20 °C the monolayers from **1**, **2**, and **3** have a liquid as well as a solid analogue state and collapse pressures between 50 and 60 mN/m. These are remarkably high values for a chain length of only nine carbon atoms. The differences in collapse areas in the surface pressure–area diagrams of these three lipids clearly demonstrate the influence of the head groups. Lipids with hydrocarbon chains and with charged head groups normally exhibit higher collapse areas then uncharged lipids due to the repulsion of the head groups. For uncharged lipids with fluorocarbon chains (e.g., **1**) the collapse areas are much higher than for analogue lipids with hydrocarbon chains (e.g., **7**; see Figure 8). If the uncharged head group (in **1**) is replaced by a charged head group in the case of fluorocarbon lipids (e.g., **2** and **3**), a decrease in collapse area is observed. A possible explanation for this reverse behavior could be ionic interactions of the head groups with the counterions in the subphase. This effect cannot be explained in detail yet and warrants further investigation.

The enhanced membrane stability of a monolayer built from a fluorocarbon amphiphile in comparison with a hydrocarbon amphiphile bearing the same head group is demonstrated in Figure 2. The monolayer of the hydrocarbon monoester of itaconic acid (**10**) shows only a liquid analogue state and has a much lower collapse pressure than the fluorocarbon monoester **4**. The monolayer of **4** exhibits both liquid and solid analogue states, although the overall chain length is two carbon atoms shorter than in **10**.

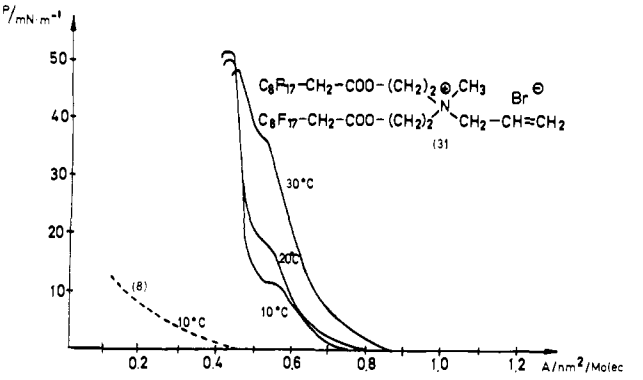

Figure 3. Temperature dependence of the surface pressure–area diagrams of the fluorocarbon lipid **3** (—) and comparison with the analogue lipid with hydrocarbon chains **8** (---) (subphase: H_2O).

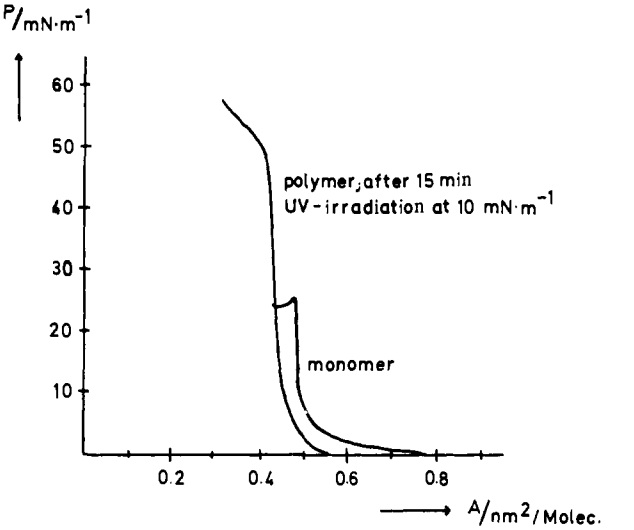

Figure 4. Surface pressure–area diagram of a monomer and polymer monolayer of **6** at 20 °C (subphase: H_2O).

In Figure 3 a comparison is made between the surface pressure–area diagrams of the fluorocarbon lipid **3** and of the hydrocarbon lipid **8** with the same head group and identical chain length. The temperature dependence of the spreading behavior of the fluorocarbon lipid **3** is also given in Figure 3.

The monolayer formed from the fluorocarbon amphiphile **3** shows a liquid and a solid analogue state and a collapse pressure of about 50 mN/m at 30 °C. In contrast, the hydrocarbon lipid **8** containing the same chain length does not form a stable monolayer even at 10 °C. This instability can be attributed to the water solubility of **8**, again demonstrating the higher hydrophobicity of the fluorocarbon chains.

Polymerization of Fluorocarbon Lipids in Monolayers. The unsaturated fluorine-containing amphiphiles **4**, **5**, and **6** could be polymerized in the monolayer with retention of orientation. The monoallyl lipid **3** could not be polymerized even with the catalyst system described by Harada et al.[12]

As in the case of hydrocarbon amphiphiles[1,13] the monolayers

(12) Harada, S.; Hasegawa, S. *Makromol. Chem., Rapid Commun.* **1984**, *5*, 27.
(13) Hupfer, B.; Ringsdorf, H. *Chem. Phys. Lipids* **1983**, *33*, 263.
(14) Büschl, R.; Hupfer, B.; Ringsdorf, H. *Makromol. Chem., Rapid Commun.* **1982**, *3*, 589.
(15) Crisp, D. J. "Surface Chemistry"; Butterworths: London, 1949; p 17.

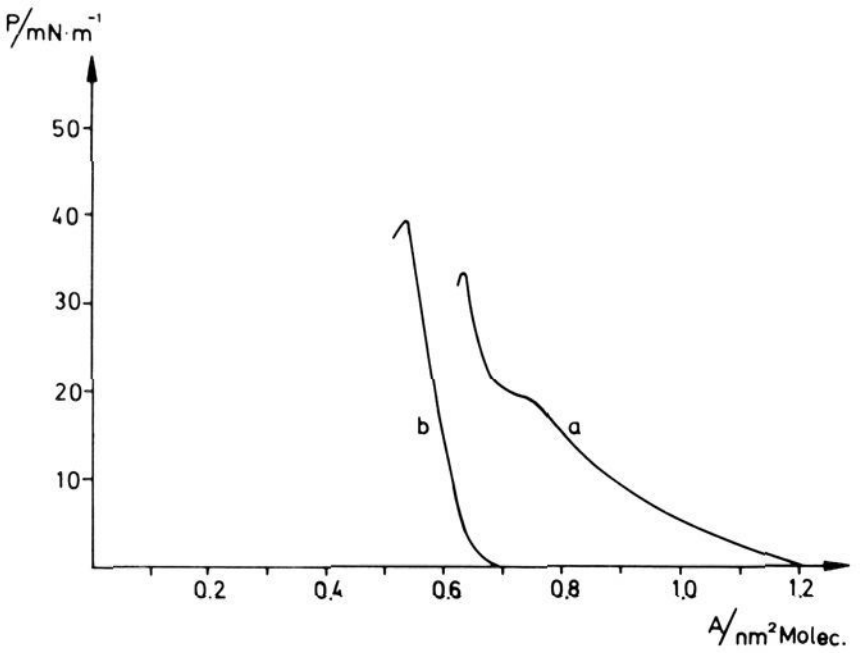

Figure 5. Surface pressure–area diagrams of monolayers of **5** (a) before polymerization and (b) after polymerization (3-h UV irradiation at 25 mN m^{-1}) at 20 °C (subphase: H_2O).

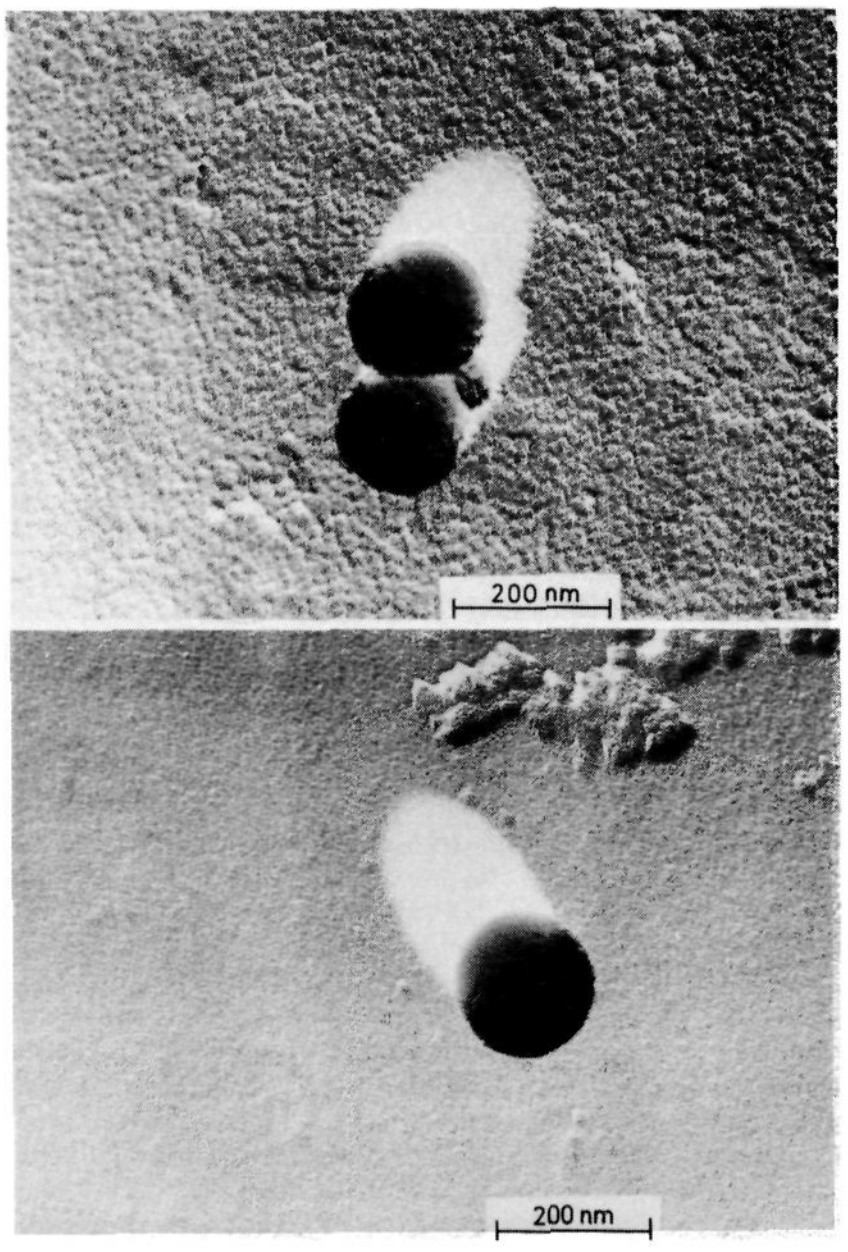

Figure 6. Electron micrograph of liposomes from **6**: (a) monomeric, (b) polymeric (after 15 min of UV irradiation).

of the polymerizable fluorocarbon lipids **5** and **6** display an increased stability after UV polymerization. This is shown in Figure 4 for the muconic acid derivative **6** where the monolayer exhibits closer packing and a higher collapse pressure after polymerization.

The typical disappearance of the liquid analogue state of a monomeric monolayer during polymerization is shown in Figure 5 for the itaconic acid derivative **5**. This polymer film also shows a higher packing density and a slightly increased collapse pressure compared to its monomer.

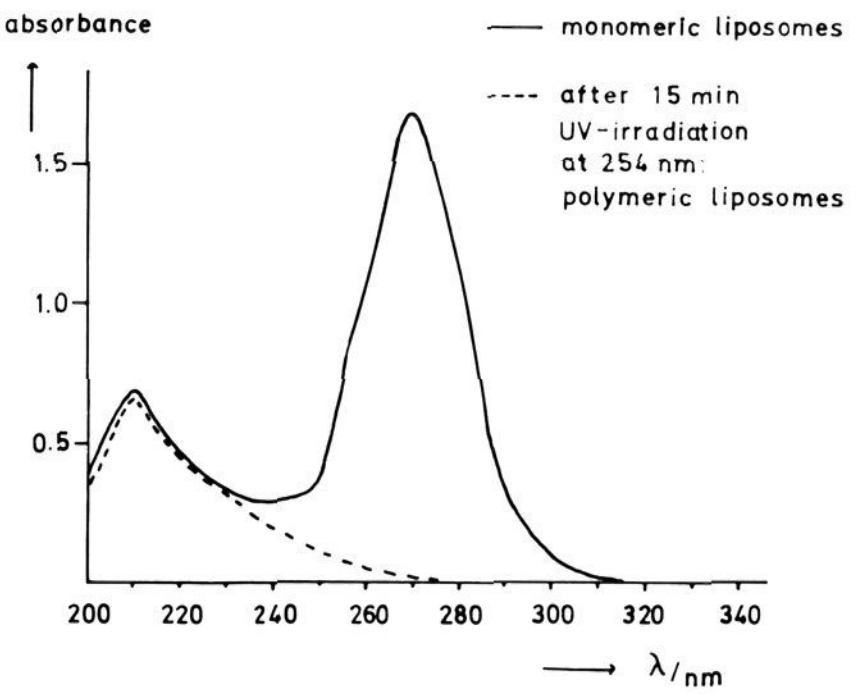

Figure 7. UV spectra of monomeric and polymeric liposomes from **6**.

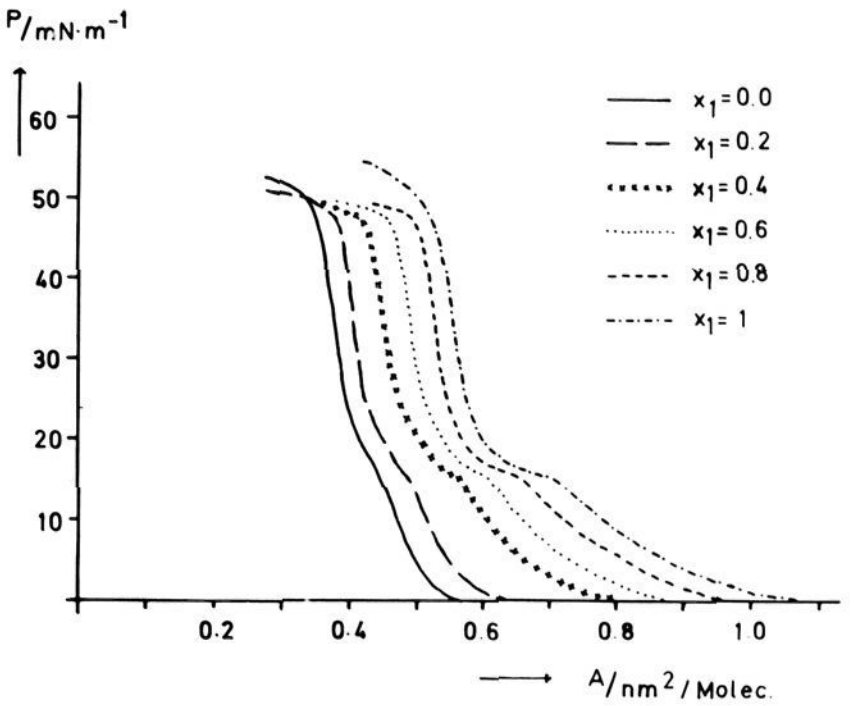

Figure 8. Surface pressure–area diagrams of monolayers of different mixtures of **1** and **7** at 20 °C (subphase: H_2O): x_1, mole fraction of **1**.

Monomeric and Polymeric Liposomes from Amphiphiles with Fluorocarbon Chains. The fluorocarbon amphiphiles with two hydrophobic chains (**1**, **2**, **3**, **5**, **6**) from liposomes upon ultrasonication in water or phosphate buffer solution. The formation of liposomes was shown by GPC and electron microscopy. To verify the formation of liposomes by GPC the vesicles were prepared in a dye solution. The dye outside the liposomes is removed by using, for example, a Sephadex G 50 column. A colored fraction in the exclusion volume indicates the existence of liposomes having the dye entrapped. Dye-containing liposomes were used to study membrane permeability and dye release.[20–26]

(16) It has to be noted that phase-transition temperatures in monolayers and double layers of liposomes cannot be compared at all. Beside the fact, that in double layers additional interactions of the hydrophobic chains are possible, the pressure in lipid double layers is not exactly know.

(17) E.g., melting enthalpy of hexane, 36.3 cal/g: Dousling, D. R.; Hoffmann, H. M. *J. Am. Chem. Soc.* **1946**, *68*, 1707. Melting enthalpy of perfluorohexane, 4.7 cal/g: Dunlap, R. D.; Hoffmann, H. M. *J. Am. Chem. Soc.* **1946**, *68*, 1708.

(18) Krbeced, R.; Gebhardt, C.; Gruler, H.; Sackmann, E. *Biochim. Biophys. Acta* **1979**, *554*, 1.

(19) Gaub, H.; Sackmann, E.; Büschl, R.; Ringsdorf, H. *Biophys. J.* **1984**, *45*, 725.

(20) Büschl, R.; Folda, T.; Ringsdorf, H. *Makromol. Chem., Suppl.* **1984**, *6*, 245.

(21) Albrecht, O.; Sackmann, E. *J. Phys. E*: **1980**, *13*, 512.

(22) Albrecht, O. *Thin Solid Films* **1983**, *99*, 227.

(23) Kleiner, E. K. (Geigy, J. R.; A.G.) Ger. Offen. 2021072 (Cl. C 07 cd. C 08 f).

(24) Milas, N. A.; Eles, D. *J. Am. Chem. Soc.* **1956**, *78*, 5903.

(25) Kippenberger, D.; Rosenquist, K.; Adberg, L.; Tundo, P.; Fendler, J. H. *J. Am. Chem. Soc.* **1983**, *105*, 1129.

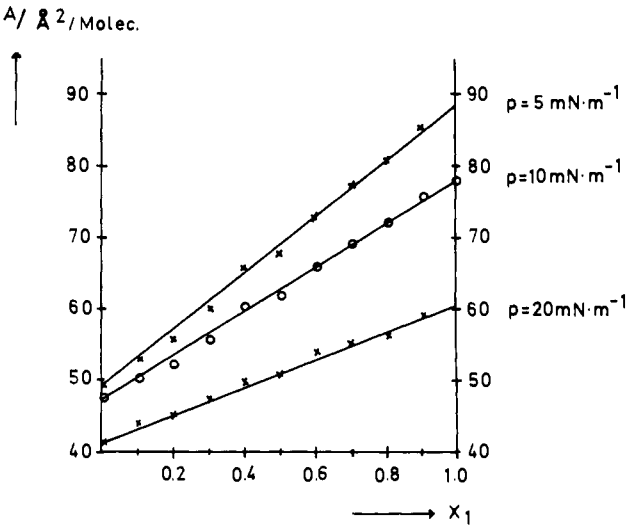

Figure 9. Mean molecular area as a function of the composition of monolayers for the system **1**/**7** at different pressures (T = 20 °C, subphase: H_2O).

Figure 6a is an EM photograph of liposomes formed from **6** which demonstrates their spherical structure.

Analogous to the reaction in monolayers, polymerization in the oriented spherical bilayer form of the liposomes occurred upon irradiation with UV light. Preservation of the spherical structure of the polymeric vesicles is demonstrated in Figure 6b. The polymerization of the liposomes could be followed by using UV spectroscopy by measuring the disappearance of the butadiene absorption band at 269 nm during UV irradiation (see Figure 7).

Mixing Behavior of Hydrocarbon and Fluorocarbon Amphiphiles in Monolayers and Liposomes. The mixing behavior of **1** and comparable hydrocarbon derivative **7** with the same head group have been investigated in monolayers. Surface pressure–area diagrams for different compositions of a two-component monolayer have been recorded (Figure 8).

The mixing behavior of polymerizable lipids with hydrocarbon chains has been investigated[14] in monolayers and can be studied by using the phase rule of Crisp.[15] The area of the mixed monolayers at defined surface pressure is plotted against the mole fraction of the mixture. For an ideal mixing behavior (complete miscibility or complete phase separation) these areas show a linear dependence on the mole fraction. Any deviation from that linearity is caused by interactions of the different amphiphiles which demonstrates at least partial miscibility. Figure 9 shows the mean area composition diagram for **1** and **7** as derived from Figure 8.

At all investigated pressures the area at a constant pressure (5, 10, 20 mN m^{-1}) is linearly dependent on the composition of the monolayer. This demonstrates the ideal behavior of these lipids. On the basis of these measurements alone one cannot distinguish between an ideal miscibility and phase-separated system for the mixture of **1** and **7** because the collapse pressures of the two pure systems are nearly equal. Thus, an additional method is necessary to distinguish between ideal miscibility and a phase-separated system.[15] As an additional method to characterize phase-separated monolayers, temperature-induced area variations at constant pressures (isobars) can be used. At the melting point the isobar of a three-dimensional system (crystal) shows an increase in volume. Similarly an increase in area is displayed in the two-dimensional monolayer system when an increase in temperature causes a phase change of the film from the solid analogue to the liquid analogue orientation. For this reason the phase-transition temperatures of monolayers of **1**, **7**, and a 1:1 mixture of both were investigated, (Figure 10).

Lipid **1** has a transition temperature of 7 °C at 10 mN m^{-1}. In contrast, the hydrocarbon amphiphile **7** exhibits a transition temperature of 45 °C at the same pressure. Both of these transitions are seen in the monolayer of a 1:1 mixture of the lipids. This demonstrates that each lipid in the two component monolayer has its own phase transition. The results from this method and the mean area composition diagrams in Figure 9 prove that a phase-separated membrane is formed from these hydrocarbon and fluorocarbon amphiphiles.

(26) Hupfer, B.; Ringsdorf, H.; Schupp, H. *Chem. Phys. Lipids* **1983**, *33*, 355.

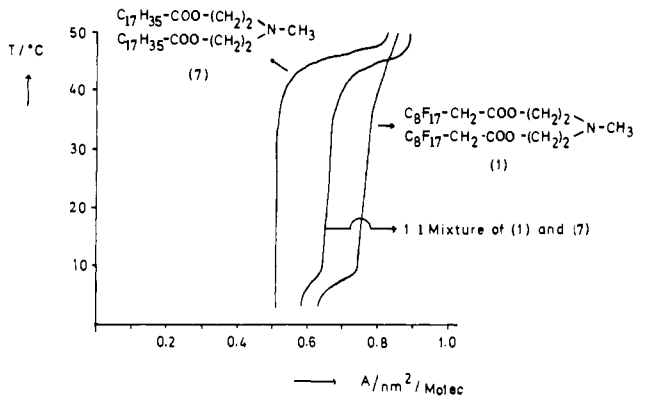

Figure 10. Isobars of **1** and **7** and a 1:1 mixture of both lipids at a pressure of 10 mN m^{-1} (subphase: H_2O).

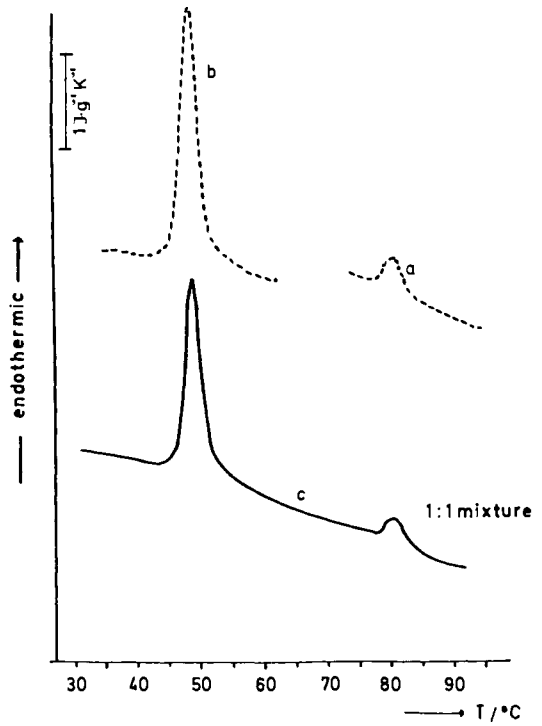

Figure 11. DSC curves of liposomes from **3** (a), **9** (b), and the 1:1 mixture of both lipids (c).

The mixing behavior of lipids with hydrocarbon and fluorocarbon chains was also investigated in liposomes. Figure 11 shows the DSC curves of liposomes from **3**, from the hydrocarbon compound **9**, and from the 1:1 mixture of both components.

When the DSC curves of liposomes prepared from **3** or **9** alone (Figure 11a,b) are compared, it can be seen that the phase-transition enthalpy of the fluorocarbon amphiphile is much lower.[16] This is in agreement with the low-melting enthalpy of fluorocarbons compared to their hydrocarbon analogues.[17] Liposomes composed of a 1:1 mixture of both lipids (Figure 11c) exhibit two transitions which are identical with the transitions found independently for liposomes of **3** or **9**. These results again demonstrate that phase separation occurs in mixtures of hydrocarbon and fluorocarbon lipids. This method cannot distinguish between the formation of two different populations of liposomes or the formation of liposomes with phase-separated membranes. An additional method used to investigate the mixing behavior of lipids in liposomes utilizes freeze-fracture electron microscopy. Natural

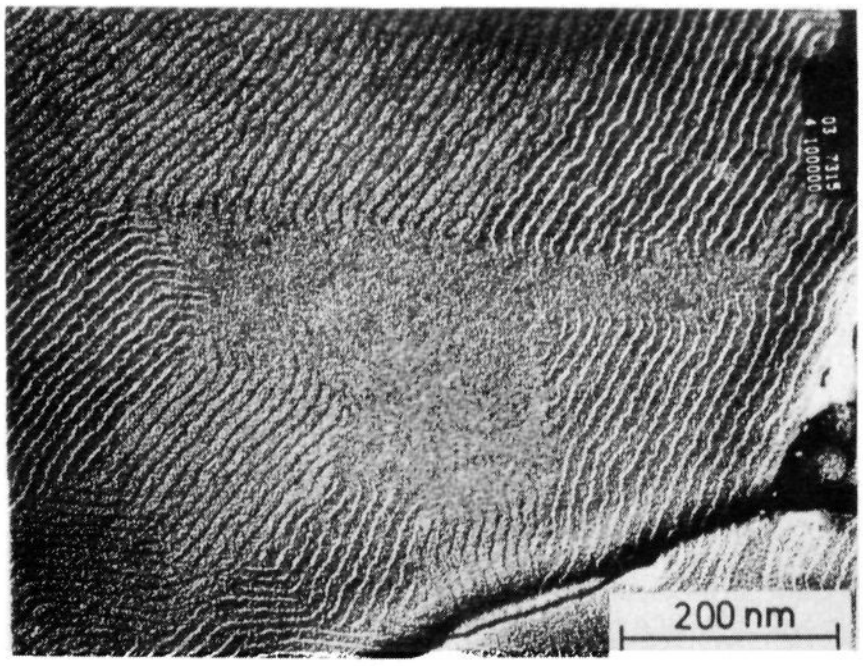

Figure 12. Freeze-fracture electron micrograph of a liposomal surface containing 95 mol % DMPC and 5 mol % **1** shock-frozen from a temperature of 17 °C after 12-h annealing at 80 °C.

lipids such as dimyristoylphosphatidylcholine (DMPC) exhibit a characteristic ripple structure when the liposomes are shock-frozen at a temperature in the pretransition range of the lipid (17 °C for DMPC).[18,19] Liposomes formed from lipids containing fluorocarbon chains (e.g., from **1**), like liposomes formed from other synthetic lipids with unnatural head groups, show a homogeneous surface when investigated by freeze-fracture electron microscopy.[19,20] Figure 12 illustrates the phase separation which occurs in mixed liposomes prepared from **1** and DMPC. The smooth surface area of the fluorocarbon lipid is surrounded by the typical ripple marks of the DMPC surface in the liposome. Relatively large phase-separated areas of about 150-nm diameter are found in mixed liposomes of DMPC containing as low as 5 mol % of **1**. This definitely proves that the two lipids form liposomes with phase-separated membranes and not just two different populations of liposomes.

In addition phase-separated mixed liposomes have been prepared in which only one of the phases was polymerized. It could be demonstrated that the unpolymerized areas could be removed from the liposome and that the liposomes are not destroyed by this procedure. The holes created in the liposome by this technique can be seen in the scanning electron micrographs.[20]

Experimental Section

General Methods. Melting points were determined with a Büschi melting point apparatus and are uncorrected. Column chromatography was performed with E. Merck silica gel 60 (0.063–0.20 mm).

Infrared (IR) spectra were obtained on a Beckmann IR-4220 spectrometer which was calibrated by using poly(styrene). The IR bands are reported in wavenumbers (cm^{-1}). Nuclear magnetic resonance (NMR) spectra were recorded on a Bruker WH-90 (90 MHz) spectrometer. Chemical shifts are reported in ppm (δ) downfield relative to tetramethylsilane (Me_4Si) and apparant coupling constants (J) are reported in hertz.

Ultraviolet spectra were recorded with a Beckmann DU-6 spectrophotometer.

Microanalyses were performed by Mycroanalyses Laboratories, Universität Mainz.

Preparation of Monolayers. Monolayers were spread from chloroform solution which had concentrations of 1 mg/mL. The films were spread on a LAUDA film balance where surface pressure and area were automatically recorded. Polymerization was carried out under an atmosphere of nitrogen via UV irradiation (254 nm) of the monolayer at the water surface. The isobars were recorded on a film balance built by Dr. Otto Albrecht[21,22] of our laboratory. This apparatus contains two Wilhelmi units as pressure-monitoring systems. The monolayers were spread at low-subphase temperatures (1 °C). At a constant pressure, the temperature of the subphase was gradually increased by using a constant heating rate. The dependence of area on temperature at constant pressure was recorded.

Preparation of Liposomes. Liposomes were prepared by ultrasonicating (5 min, 20 W) dispersion (1 mg/mL) of the lipids in water or phosphate buffer solution at 80 °C (Branson sonifier Model B 15). Polymerization was achieved by UV irradiation of solutions which had been previously purged with nitrogen.

Electron Microscopy Studies. Liposomes used for freeze-etching electron microscopy were prepared in a different way. Lipid films were deposited on the glass wall of a flask by evaporating a chloroform solution of the lipid or lipid mixtures (2 mg of lipid) with a rotoevaporator. Water (5 mL) or buffer solution was added and the flask was heated to 80 °C for about $^1/_2$ h. The flask was rotated for 5–10 min at 80 °C. In this way relatively large (2–4 μm) liposomes can be prepared. A portion of the sample was placed between gold plates and shock-frozen by immersion into liquid propane. The sample was then fractured and etched by using a Balzers unit.[21]

Electron microscopy measurements were carried out by using a Phillips EM 300 electron microscope after shadowing with Pt–carbon at 45 °C. Water was purified by distillation and filtration through a "Milli-Q" water filtration system (Millipore).

GPC. Methods to verify the formation of liposomes by GPC have been described previously.[26,20] The liposomes are prepared in a solution of a fluorescence dye (e.g., eosin, 6-carboxyfluorescein) having such a high concentration (approximately 0.05 m) that the dye exhibits self-quenching. The dye outside the vesicles is then removed on a Sephadex G 50 column. A colored fraction in the exclusion volume indicates the existence of liposomes which have the fluorescence dye entrapped in their aqueous interior. These liposomes can be used to investigate leakage behavior via fluorescence measurements.[20,26]

Differential Scanning Calorimetry (DSC). Liposomes for DSC measurements were prepared by ultrosonicating (3 min/20 W) dispersions (10 mg/mL) of the lipids in water at 80 °C. The thermal behavior of the compound was investigated by using a DSC-20 differential scanning calorimeter (Perkin-Elmer). The scan rate was 2.5 K/min.

Materials. 1*H*,1*H*,2*H*,2*H*-Perfluorododecanol and perfluorooctylacetyl chloride were purchased by Riedel-de Haen AG. 1*H*,1*H*-Perfluorooctylamine was obtained from BASF. 1*H*,1*H*,11*H*-Perfluoroundecanol was obtained from Ventron. Itaconic anhydride, allyl bromide, methyl bromide, and *N*-methyldiethanolamine were obtained from EGA-Chemie. *N*,*N*-Bis(2-hydroxyethyl)-2-aminoethanesulfonic acid was purchased from Roth. *N*,*N*′-Dicyclohexylcarbodiimide, 4-(dimethylamino)pyridine, and muconic acid were purchased from Aldrich. All solvents used were analytical grade and dried with molecular sieves (Merck).

Synthesis of the Fluorocarbon Amphiphiles. *N*,*N*-Bis[2-(((perfluorooctyl)acetyl)oxy)ethyl]-*N*-methylamine, 1. **1** was synthesized by refluxing 0.48 g (4 mmol) of *N*-methyldiethanolamine with 4.22 g (8.5 mmol) of perfluorooctylacetyl chloride and 0.45 g (4.5 mmol) of triethylamine in dry chloroform (50 mL) for 1 h. This reaction mixture was filtered and the filtrate was evaporated. The crude reaction product was dissolved in ether (200 mL) and washed three times with saturated sodium bicarbonate. The organic phase was dried (Na_2SO_4) and the solvent was evaporated. Recrystallization twice from methanol/ether (1:1) gave **1** as a white crystalline solid: yield 1.7 g (41%); mp 38 °C; ^{1}H NMR (CD_3OD) δ 2.38 (s, 3 H, CH_3–N), 2.82 (m, 4 H, CH_2–N), 3.49 (t, J = 18.5 Hz, 4 H, CF_2–CH_2), 4.59 (m, 4 H, COO–CH_2); IR (KBR) 1730 (CO), 1210, 1150 (CF) cm^{-1}. Anal. Calcd for $C_{25}H_{15}O_4NF_{34}$: C, 28.89; H, 1.45; N, 1.35. Found: C 28.69; H, 1.21; N, 1.56.

***N*,*N*-Bis[2-(((perfluorooctyl)acetyl)oxy)ethyl]-*N*-dimethylammonium Bromide, 2.** The long-chain amine **1** (1.04 g, 1 mmol) was quaternized with excess methyl bromide (0.5 g) in ether (50 mL) by stirring at 0 °C for 12 h. The precipitate was isolated: yield 0.95 g (84%); mp 124 °C; ^{1}H NMR ($(CD_3)_2CO$) δ 3.2–3.7 (m, 14 H, $(CH_2)_2N$, $N(-CH_3)_2$, CF_2–CH_2), 4.32 (t, 4 H, COO–CH_2); IR (KBr) 1730 (CO) 1205, 1145 (CF) cm^{-1}. Anal. Calcd for $C_{26}H_{18}O_4NF_{34}Br$: C, 27.54; H, 1.60; N, 1.24. Found: C, 27.25; H, 1.79; N, 1.44.

***N*,*N*-Bis[2-(((perfluorooctyl)acetyl)oxy)ethyl]-*N*-methyl-*N*-allylammonium Bromide, 3.** **3** was synthesized by refluxing 1 g (0.96 mmol) of **1** with 1.16 g (9.6 mmol) of allyl bromide in acetonitrile (30 mL) for 1 h. After the solvent and unreacted bromide were removed in vacuo, the product was recrystallized twice from methanol/ether (1:1): yield 0.6 g (55%); mp 160–161 °C; ^{1}H NMR (CD_3OD) δ 3.22 (s, 3 H, CH_3—N), 3.52 (t, J = 18.5 Hz, 4 H, CF_2—CH_2), 3.89 (m, 4 H, CH_2—N), 4.71 (m, 4 H, COO-CH_2), 4.20 (d, 2 H, N—CH_2—CH), 5.6-6.2 (m, 3 H, CH=CH_2); IR (KBr) 1730 (CO), 1630 (C=C), 1210, 1150 (CF) cm^{-1}. Anal. Calcd for $C_{28}H_{15}NO_4F_{34}Br$: C, 28.98; H, 1.74; N, 1.21. Found: C, 28.92; H, 1.74; N, 1.33.

1*H*,1*H*,2*H*,2*H*-Perfluorododecyl Itaconate, 4. **4** was prepared by refluxing a mixture of 0.5 g (4.5 mmol) of itaconic anhydride and 2.3 g (4 mmol) of 1*H*,1*H*,2*H*,2*H*-perfluorododecanol in toluene (30 mL) for 5 h in the presence of 100 mg of anhydrous $ZnCl_2$ (added as a solution of 3 mL of acetone). The mixture was filtered, and when the mixture was cooled in an ice bath the product was separated as a white solid: yield 1.7 g (63%); mp 116 °C; ^{1}H NMR (CD_3OD) δ 2.2–2.8 (m, 2 H,

CH_2—CF_2), 4.40 (t, 2 H, COO—CH_2), 3.28 (s, 2 H, CH_2—CO), 6.0 (m, 2 H, CH_2=C); IR (KBr) 1745, 1700 (CO), 1645 (C=C), 1230, 1160 (CF) cm^{-1}. Anal. Calcd for $C_{17}H_9O_4F_{21}$: C, 30.20; H, 1.34. Found: C, 30.41; H, 1.47.

Bis(1*H*,1*H*-perfluorooctyl)itaconamide, 5. The synthesis of **5** is described elsewhere.[23]

***N*,*N*-Bis(((2,2,3,3,4,4,5,5,6,6,7,7,8,8,9,9,10,10-eicosafluoroundecyl)-muconyl)ethyl)taurine, 6.** 1*H*,1*H*,11*H*-Eicosafluoroundecanol (10.64 g, 0.02 mol) was added slowly to a refluxing solution of 3.58 g (0.02 mol) of *trans,trans*-muconyl chloride[24] in dry chloroform (200 mL). After 3 h the chloroform was evaporated and the residue was distilled in vacuo. The resulting monoester monoacid chloride has a boiling point of 110 °C (0.03 torr): yield 9.85 g (73); mp 76-78 °C. **6** was obtained by refluxing 3.37 g (5 mmol) of the above hexadienoic acid mono 1*H*,1*H*,11*H*-eicosafluoroundecanoyl ester monoacid chloride with 0.53 g (2.5 mmol) of *N*,*N*-bis(2-hydroxyethyl)-2-aminoethanesulfonic acid in dry chloroform (600 mL) for 3 days. Purification of the crude product was achieved by repeated recrystallization from chloroform: yield 2.5 g (67%); mp 108 °C; ^1H NMR ($CDCl_3$) δ 2.7-3.6 (m, 8 H, $(CH_2)_2NCH_2CH_2SO_3$), 4.2 (br t, 4 H, $COOCH_2$), 4.64 (t, 4 H, J = 15 Hz, CF_2—CH_2), 6.03 (t, 2 H, J = 50 Hz, t, H—CF_2), 6.11-6.41 (m, 2 H, CH—COO), 7.20-7.48 (m, 2 H, CH—C—COO); IR (KBr) 1736 (CO), 1619, 1594 (C=C), 1203 (CF) cm^{-1}. Anal. Calcd for $C_{40}H_{27}O_{11}NSF_{40}$: C, 32.25; H, 1.81; N, 0.94, Found: C, 31.97; H, 1.63; N, 0.77.

Synthesis of the Comparable Hydrocarbon Compounds. For the synthesis of **7**, 13.4 g (65 mmol) of dicyclohexylcarbodiimide dissolved in dry chloroform (150 mL) was added to a solution of 14.2 g (50 mmol) of steric acid, 3 g (25 mmol) of bis(2-hydroxyethyl)methylamine, and 100 g of (dimethylamino)pyridine in dry chloroform (200 mL) at 0 °C. After the solution was stirred for 12 h at room temperature the urea was separated by filtration. The solution was washed 3 times with saturated sodium bicarbonate and with water. The crude reaction product was purified by liquid chromatography on silica gel by using methylene chloride as eluent and then recrystallized from ether: yield 10.6 g (65%); mp 49 °C; ^1H NMR ($CDCl_3$) δ 0.89 (t, 6 H, C-CH_3), 1.25 (br s, 60 H, $(CH_2)_{15}$), 2.25 (t, 4 H, CH_2-COO), 2.40 (s, 3 H, N-CH_3), 2.72 (t, 4 H, CH_2-N), 4.18 (t, 4 H, COO-CH_2); IR (KBr) 1735 (CO) cm^{-1}. Anal. Calcd for $C_{41}H_{81}NO_4$: C, 75.52; H 12.52; N, 2.15, Found: C, 75.23; H, 12.22, N, 1.96.

9 was synthesized as described by Fendler et al.[25] The same procedure was used to synthesized **8**. **10** was synthesized by the method described for **4**: yield 83%; mp 79-80 °C; ^1H NMR (CD_3OD) δ 0.89 (t, 3 H, CH_3), 1.28 (br, 24 H, $(CH_2)_{12}$), 3.27 (s, 2 H, CH_2—COO), 4.14 (t, 2 H, COO—CH_2), 6.01 (m, 2 H, CH_2=C); IR (KBr) 1730, 1692 (CO), 1640 (C=C) cm^{-1}. Anal. Calcd for $C_{19}H_{34}O_4$: C, 69.94; H, 10.43. Found: C, 69.61; H, 10.71.

Registry No. 1, 92844-67-2; **2**, 92844-68-3; **3**, 92844-69-4; **4**, 92844-70-7; **5**, 29883-10-1; **6**, 92844-71-8; **7**, 13998-76-0; **8**, 92844-72-9; **9**, 84454-87-5; **10**, 25328-98-7; $(HOCH_2CH_2)_2NMe$, 105-59-9; $CF_3(CF_2)_7CH_2C(O)Cl$, 64018-23-1; $H(CF_2)_{10}CH_2OH$, 307-70-0; $H(CF)_{10}CH_2OC(O)CH$=CHCH=CHC(O)Cl, 92844-73-0; $(HOCH_2CH_2)_2N(CH_2)_2SO_3H$, 10191-18-1; $CF_3(CF_2)_9(CH_2)_2OH$, 865-86-1; $CH_3(CH_2)_{13}OH$, 112-72-1; stearic acid, 57-11-4; *trans,trans*-muconyl chloride, 58823-55-5; itaconic anhydride, 2170-03-8.

Spin Distributions in Bridged Bis(cyclooctatetraene) Anion Radicals. Dicyclooctatetraenylmethane and Dicyclooctatetraenyldimethylsilane

Luis Echegoyen,*† Rene Maldonado, Jaime Nieves,† and Antonio Alegria‡

Contribution from the Departments of Chemistry, University of Miami, Coral Gables, Florida 33124, and University of Puerto Rico, Humacao Campus, Humacao, Puerto Rico 00661. *Received March 23, 1984*

Abstract: The title compounds as well as some of their alkyl-deuterated derivatives and 1,2-dicyclooctatetraenylethane were synthesized and reduced with alkali metals in hexamethylphosphoramide (HMPA). The anion radical of COT-$(CH_2)_2$-COT has the spin density localized in one of the two COT rings as evidenced by the coupling constants observed: a_{2H} = 2.55 G, a_{4H} = 2.00 G, and a_{3H} = 4.37 G. These values are very similar to those measured for *n*-butylcyclooctatetraene. The anion radical of COT-CH_2-COT exhibits a totally different ESR spectrum where the spin density is clearly delocalized over the two COT moieties, with coupling constants a_{4H} = 4.03 G, a_{2H} = 3.30 G, and a_{8H} = 0.73 G. No hyperfine interaction was observed to occur with the bridging methylene, since the ESR spectrum of $(COT-CD_2-COT)^{-\cdot}$ was identical with that of the undeuterated compound. Comparison of the ESR spectrum of $(COT-CH_2-COT)^{-\cdot}$ with that previously reported for $(COT-COT)^{-\cdot}$ shows that the molecular orbital symmetry is similar, but the energy ordering of the two HOMO's is reversed. Conjugation between the two COT rings via an interannular interaction results in spin delocalization over the entire molecule while the methylene splitting is not observable. This conjugation is not possible for $(COT-Si(CH_3)_2-COT)^{-\cdot}$ where the spin is clearly localized in only one ring: a_{4H} = 5.13 G and a_{3H} = 1.25 G. These values have been used to determine the orbital degeneracy splitting of the COT by the -$Si(CH_3)_2$-COT substituent (ϵ = -0.82 kcal/mol). This value is the highest ever reported for any substituent on a COT system.

Electrochemical and chemical reduction of cyclooctatetraene (COT) and substituted COT's have been widely investigated for many years.[1-3] The anion radical of COT has been shown to undergo electron exchange only with the dianion, since exchange between the anion radical and the neutral molecule is slow due to the required flattening of the ring upon one electron reduction.[4] This is the same reason why electrochemical reduction shows an electrochemically irreversible first wave for the formation of the anion radical followed by a reversible one leading to the formation of the aromatic (in the Hückel sense) dianion.[5] That the anion radical and dianion of COT can be formed at all is itself a re-

†University of Miami.
‡University of Puerto Rico.

(1) Allendoerfer, R. D.; Rieger, P. H. *J. Am. Chem. Soc.* **1965**, *87*, 2336.
(2) Huebert, B. J.; Smith, D. E. *J. Electroanal. Chem.* **1971**, *31*, 333.
(3) Anderson, L. B.; Hanson, J. F.; Paquette, L. A.; Kakihana, T. *J. Am. Chem. Soc.* **1971**, *93*, 161.
(4) Stevenson, G. R.; Valentin, J.; Williams, E.; Caldwell, G.; Alegria, A. *J. Am. Chem. Soc.* **1979**, *101*, 515.
(5) Fry, A. J. "Synthetic Organic Electrochemistry"; Harper and Row: New York, 1972.

0002-7863/84/1506-7692$01.50/0